

Consistent Cross-view Matching for Unsupervised Person Re-identification

Xueping Wang, Rameswar Panda, Min Liu, and Amit K Roy-Chowdhury, *Fellow, IEEE*

Abstract—Most existing unsupervised person re-identification methods focus on learning an identity discriminative feature embedding for efficiently representing images of different persons. However, higher-order relationships across the entire camera network are often ignored leading to contradictory outputs when the results of different camera pairs are combined. In this paper, we address this problem by proposing a consistent cross-view matching framework for unsupervised person re-identification by exploiting more reliable positive image pairs in a camera network. Specifically, we first construct a bipartite graph for each pair of cameras, in which each node denotes a person, and then graph matching is used to obtain optimal global matches across camera pairs. Thereafter, loop consistent and transitive inference constraints are introduced into the cross-view matches, which consider similarity relationships *across the entire camera network* to increase confidence in the matched/non-matched pairs. We then train distance metric models for each camera pair using the reliably matched image pairs. Finally, we embed the cross-view matching method into an iterative updating framework that iterates between the consistent cross-view matching and the cross-view distance metric learning. We demonstrate the superiority of the proposed method over the state-of-the-art unsupervised person re-identification methods on three benchmark datasets such as Market1501, MARS and DukeMTMC-VideoReID datasets.

Index Terms—Unsupervised person re-identification, Consistent constraints, Cross-view matching, Distance metric learning

I. INTRODUCTION

PERSON re-identification (re-id) is a cross-camera instance retrieval problem [1], [2] which aims at searching persons across multiple non-overlapping cameras. Although person re-identification has been extensively studied during the past few years, most of these methods, in particular deep learning-based methods[3], [4], [5], [6], [7], [8], [9], [10], [11], [12], [13], adopt a costly training phase that requires a large number of manually labeled cross-camera matched image pairs to learn the effective feature representation or distance metric models. These methods have shown impressive results, but their performance largely depends on huge amount of labeled samples which are difficult to collect in many real world applications. On the other hand, unsupervised learning-based person re-id methods have drawn a great deal of attention in

Xueping Wang and Min Liu are with the College of Electrical and Information Engineering at Hunan University, Changsha, Hunan, China.

Amit K Roy-Chowdhury and Rameswar Panda are with the Department of Electrical and Computer Engineering at the University of California, Riverside.

E-mails: (wang_xueping@hnu.edu.cn, rpanda002@ucr.edu, liu_min@hnu.edu.cn, amitrc@ece.ucr.edu)

This work was done while Xueping Wang was a visiting student at UC Riverside.

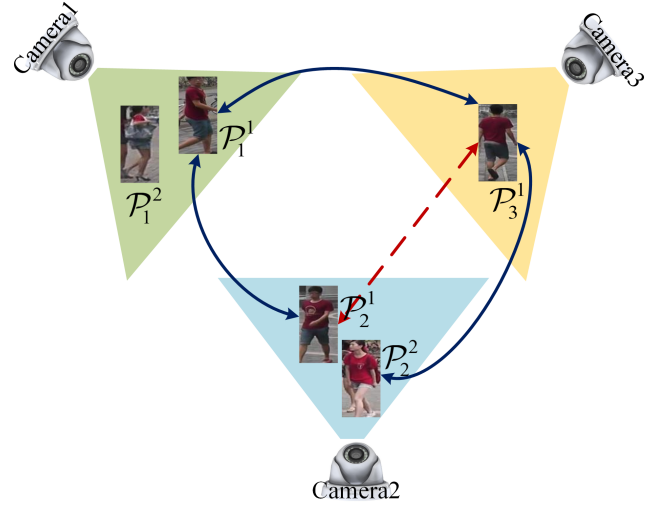


Fig. 1. An illustrative example of the contradictory matching involving 2 persons in 3 cameras. \mathcal{P}_1^1 denotes that person 1 captured in camera 1. The solid lines are the graph matching results and the dashed line is a transitive inference. We can obtain the association $(\mathcal{P}_1^1, \mathcal{P}_2^1)$, $(\mathcal{P}_1^1, \mathcal{P}_3^1)$ and $(\mathcal{P}_2^2, \mathcal{P}_3^1)$. When combining them together, we can infer that \mathcal{P}_2^1 and \mathcal{P}_3^1 are matched which leads to an infeasible scenario that indicates that \mathcal{P}_2^1 and \mathcal{P}_2^2 are the of same person. Best viewed in color.

the last few years as they do not require the labeled person identities in the feature learning or model training procedure [14], [15], [16], [17], [18], [19], [20].

Traditional unsupervised person re-identification methods concentrate on designing hand-crafted feature representations, saliency and/or dictionary learning, etc.[14], [19], [20]. In recent years, researchers are trying to incorporate deep convolutional neural networks into the unsupervised person re-identification problem to learn an identity discriminative feature embedding [15], [16], [17] to alleviate the problem of the insufficient labeled samples to some extent. However, performance of these methods are still significantly weaker compared to supervised alternatives as they fail to exploit the similarity relationships between image pairs while learning the model. Specifically, the lack of cross-view pairwise labeled data makes the learned models fail to address the significant visual appearance variations while matching persons across cameras [18].

Most existing label estimation methods for unsupervised person re-identification are based on an assumption that all the samples are distributed in the same discriminative space [16], [15], [21], [22], which is not always true for the person re-id task due to the distribution bias in different cameras

caused by the large cross-camera variations. These methods just pay attention to intra-camera or inter-camera information, which ignores the similarity relationships across a camera network by not considering the consistency of the estimated labels. This may lead to contradictory outputs when matching results from different camera pairs are combined. As shown in Figure 1, by the using of cross-view matching methods, we can obtain the matching associations between $(\mathcal{P}_1^1, \mathcal{P}_2^1)$, $(\mathcal{P}_2^2, \mathcal{P}_3^1)$ and $(\mathcal{P}_1^1, \mathcal{P}_3^1)$ independently. However, when these matches from different camera pairs are combined, it leads to an infeasible scenario - \mathcal{P}_1^1 and \mathcal{P}_2^2 are the same person. It is hard to distinguish which matching is reliable [23], [24], [3]. *So can we develop a more reliable cross-camera label estimation strategy by exploiting the consistent similarity information in a network for further improving the recognition performance of unsupervised person re-identification?* This is an especially important problem in the context of many person re-identification systems involving large number of cameras.

To address the above problem, in this paper, we propose a consistent cross-view matching framework for unsupervised person re-identification, which introduces loop consistent and transitive inference consistent constraints as shown in Figure. 2. In particular, a bipartite graph is first constructed for each pair of cameras and then a graph matching method via Hungarian algorithm is employed to obtain optimal cross-view matches across pairwise cameras. Loop consistent and transitive inference consistent constraints are then introduced into the pairwise matches, including a definition for the reliability of the cross-view matching to reduce the false positive matches. Distance metrics are then learned for each pair of cameras using the obtained reliable matched image pairs. Finally, our consistent cross-view matching method is incorporated into an iterative updating framework which iterates between the consistent cross-view matching and the cross-view distance metric learning.

To summarize, the contributions of our work are as follows.

- We propose a consistent cross-view matching framework for unsupervised person re-identification by iterating between consistent cross-view matching and distance metric learning. On one hand, we obtain the reliable cross-camera matched image pairs with a guarantee of the consistent constraints and on the other hand, we learn effective distance metric models across camera pairs using the corresponding cross-view matches for efficient person re-identification in a camera network.
- We introduce a definition for reliability of the cross-view matched image pairs by introducing loop consistent and transitive inference consistent constraints into the cross-view matching. By balancing the performance between the quality and quantity of the estimated matches, we can reduce the incorrect matches significantly and enhance the robustness of the cross-view matches against the outliers captured by different cameras.
- Extensive experiments demonstrate that our approach significantly outperforms the state-of-the-art unsupervised person re-identification methods by a large margin on Market1501, MARS and DukeMTMC-VideoReID dataset with variable number of cameras.

II. RELATED WORK

We now describe the previous works relevant to the method discussed in this paper, including unsupervised person re-identification and cross-view matching for re-identification.

A. Unsupervised Person Re-identification

Unsupervised learning models have recently received much attention in person re-identification as they did not require manually labeled data. One of the key factors in unsupervised methods is to obtain effective and reliable samples to train a model from the massive unlabeled dataset. Fan et al. [16] proposed a k -means clustering-based method to select reliable images gradually and use them to fine tune a deep neural network to learn discriminative features for person re-identification. Xia et al. [15] proposed a hierarchical clustering-based feature embedding method by regarding sample labels as supervision signals to train a non-parametric convolutional neural network [25]. Liu et al. [26] presented a person re-identification method which iterates between cross-camera tracklet association and feature learning. Yu et al. [17] proposed a soft multilabel learning method by comparing the unlabeled person images with a set of known reference person images from an auxiliary domain to predict the soft label for each target image. Li et al. [18] proposed a deep learning based tracklet association method by jointly learning per-camera tracklet association and cross-camera tracklet correlation to obtain the label information. Zhong et al. [27] exploited the underlying invariance in domain adaptive person re-identification to reduce the feature distribution gap between labeled source domain and unlabeled target domain. Ye et al. [21] proposed a dynamic label graph matching method (DGM) for cross-camera label estimation to obtain pairwise similarity information across camera pairs for unsupervised person re-identification. Generative adversarial networks have also been adopted to train a camera style transfer model to bridge the gap between the labeled source domain and unlabeled target domain [28], [29]. In contrast to DGM, our consistent cross-view matching method utilizes loop consistent and transitive inference consistent constraints including a definition for reliability of the cross-view matching such that the matched image pairs are more robust against the inaccurate and noisy matches caused by the large variance between different cameras.

B. Cross-view Matching for Person Re-identification

Graph matching has been widely used in computer vision and machine learning domains, such as shape matching and object recognition [30], [31]. Recently, several works also introduce it into the person re-identification task. Ye et al. [22] presented a dynamic graph co-matching method to obtain the corresponding image pairs across cameras by fully utilizing the abundant image frames within the video sequences but they fail to consider the consistency of the matches across the camera network. Das et al. [23], [24] proposed a consistent re-identification method in a camera network by considering the matching consistency to improve camera pairwise re-identification performance. However, the

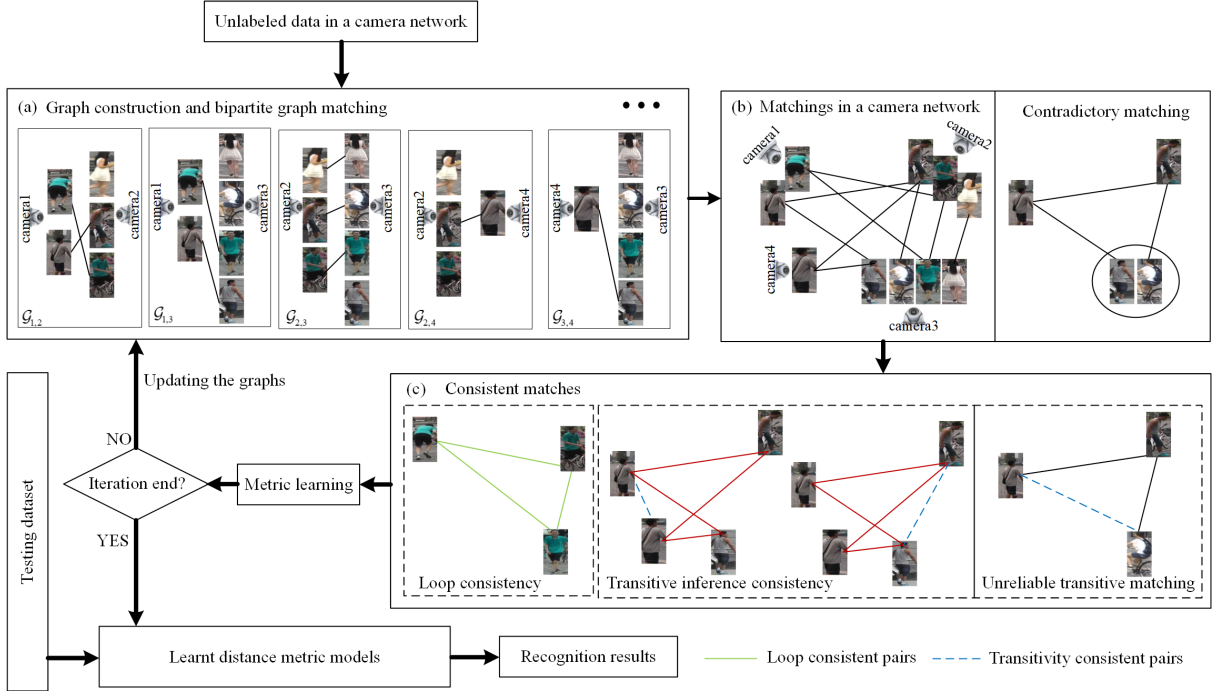


Fig. 2. Overview of our proposed method for consistent cross-view matching in person re-identification. (a) graph construction for each pair of cameras in a camera network with 4 cameras and bipartite graph matching for cross-camera label estimation. Note that only part of the matches are shown in figure; (b) pair-wise matches in a camera network which show contradictory matches across different images; (c) consistent matches by introducing loop consistent and transitive inference consistent constraints for reducing the false positives caused by the direct graph matching. By considering the reliability of the matches, we can further reduce the unreliable transitive matches. Finally, we use the consistent matches to iteratively train a distance metric model for each graph and update the graphs using the learned models.

network consistent person re-identification approach is directly utilized in the recognition procedure and not employed in the training stage, which is not suitable for large-scale datasets. Following [23], Lin et al. [3] proposed a consistent-aware deep learning method by incorporating consistent constraints into deep learning framework for person re-identification. However, they require massive labeled images to train the model. Roy et al. [32] constructed a k -partite graph for the camera network and then exploited transitive information across the graph to select an optimal subset of image pairs for manual labeling. However, the approach in [32] needs human in the loop to label the selected samples. Li et al. [33] proposed an unsupervised representation learning method by considering graph-based consistent constraints, in which they select positive pairs by loop consistency and hard negative pairs by geodesic distance. However, the k -NN based consistency constraints are not suitable for the person re-identification problem because of the large variations across different cameras. Yan et al. [34], [35] proposed a unified alternating optimization framework for robust and consistent multi-graph matching. Different from these works, our approach considers both loop consistency and transitive inference consistency for measuring the reliability of the cross-view matches while selecting the reliable image pairs, and we train distance metric model for each camera pair, which will reduce the negative effect caused by the large variance of the conditions encountered in a camera network.

III. CONSISTENT CROSS-VIEW MATCHING

The proposed consistent cross-view matching framework is comprised of three steps. First, a graph matching is employed to obtain the optimal cross-view matches over all camera pairs. Second, consistency constraints (loop consistent constraints and transitive inference consistent constraints) are introduced to measure the reliability of the pairwise matches in a camera network. Finally, we iteratively refine the graph structure with better similarity measurements learned from the reliable matching pairs.

A. Graph Matching

The consistent cross-view matching starts with the cross-camera pairwise matching associations between the targets. In this subsection, we give a brief description of the process, in which cross-camera pairwise matching associations are generated. Let there be R cameras in a network. The number of possible camera pairs is $\binom{R}{2} = \frac{R \cdot (R-1)}{2}$ and we construct a bipartite graph for each pair of cameras.

1) *Vertex*: We represent each camera r as a vertex set V_r with n_r vertices. Each vertex in the vertex set V_r denotes a person captured by this camera, $V_r = \{\mathcal{P}_r^1, \mathcal{P}_r^2, \dots, \mathcal{P}_r^{n_r}\}$. Specifically, vertex \mathcal{P}_r^i represents the i^{th} person captured in r^{th} camera. We construct a bipartite graph $\mathcal{G}_{p,q} = \{V_p, V_q\}$ for each pair of cameras (p, q) , in which each vertex denotes a person. Note that we will use the terms ‘person’ and ‘vertex’ interchangeably throughout our work.

2) *Matching cost matrix*: Let $C_{p,q}$ denote the matching cost matrix between camera p and camera q . The cell $c_{p,q}^{i,j}$ in the matching cost matrix $C_{p,q}$ denotes the matching cost between the persons \mathcal{P}_p^i and \mathcal{P}_q^j . We calculate the matching cost $c_{p,q}^{i,j}$ with the distance, $c_{p,q}^{i,j} = D_{M_{p,q}}(\mathcal{P}_p^i, \mathcal{P}_q^j)$, where $M_{p,q}$ is the corresponding distance metric learned using the selected image pairs (initialized with identity matrix before the learning).

3) *Assignment matrix*: We use the assignment matrix $X_{p,q}$ to represent the matching associations between the persons across camera pairs, one for each camera pair. Each element $x_{p,q}^{i,j}$ of the assignment matrix $X_{p,q}$ between the camera pair (p, q) represents the matching association of the person \mathcal{P}_p^i and \mathcal{P}_q^j which is defined as follows:

$$x_{p,q}^{i,j} = \begin{cases} 1, & \text{if } \mathcal{P}_p^i \text{ and } \mathcal{P}_q^j \text{ are the same person;} \\ 0, & \text{otherwise.} \end{cases} \quad (1)$$

4) *Cross-view matching*: Ideally, the same n persons are present in each of the camera in a camera network. As a result, the assignment matrix $X_{p,q}$ is a permutation matrix, i.e., only one element per row and per column is 1, all the others are 0. Mathematically, $\forall x_{p,q}^{i,j} \in \{0, 1\}$

$$\sum_{j=1}^n x_{p,q}^{i,j} = 1, i = 1, 2, \dots, n \text{ and } \sum_{i=1}^n x_{p,q}^{i,j} = 1, j = 1, 2, \dots, n \quad (2)$$

To compute the matching associations across camera pairs, we follow [21], [23] to formulate it as a binary linear programming with linear constraints:

$$\begin{aligned} \arg \min_{\substack{x_{p,q}^{i,j} \\ i,j=1,\dots,n}} \sum_{i,j=1}^n c_{p,q}^{i,j} x_{p,q}^{i,j} \\ \text{subject to: } & x_{p,q}^{i,j} \in \{0, 1\}, \forall i, j = 1, \dots, n \\ & \sum_{i=1}^n x_{p,q}^{i,j} = 1, \forall j = 1, \dots, n \\ & \sum_{j=1}^n x_{p,q}^{i,j} = 1, \forall i = 1, \dots, n \end{aligned} \quad (3)$$

By using the bipartite graph matching method, we can obtain a set of the optimal assignment matrices across the pair of cameras, $\mathbf{X} = \{X_{p,q} | p, q = 1, 2, \dots, R, p < q\}$, where $X_{p,q} = \{x_{p,q}^{i,j} | i, j = 1, 2, \dots, n\}$.

B. Consistent Cross-view Matching

In a large camera network, different cameras capture very different persons. Therefore, it is common that one camera may not capture every person. In this situation, a person from any camera p can have at most one matching from another camera q . In other words, the matching association values in every row or column of the assignment matrix can all be 0. As a result, the matching association constraints can now be changed as follows:

$$\sum_{j=1}^{n_q} x_{p,q}^{i,j} \leq 1, i = 1, 2, \dots, n_p \text{ and } \sum_{i=1}^{n_p} x_{p,q}^{i,j} \leq 1, j = 1, 2, \dots, n_q \quad (4)$$

where n_p and n_q are the number of persons in camera p and camera q , respectively. With this generalization, the previous

cross-view matching method is no longer valid as the optimal solution generated by the graph matching-based method will try to get as many matching associations as possible across camera pairs. Thus, the assignment matrix may contain a lot of false positive matches. In addition, direct cross-view matches ignore the similarity relationships across a camera network by not considering the consistency of the matched image pairs across the camera pairs in a network. It may lead to contradictory outputs when these matching associations from different camera pairs are combined [23], as shown in Figure 1. To address this problem, we introduce both loop consistency and transitive inference consistency into the bipartite graph matching, as shown in Figure 3.

1) *Indirect matching*: The direct matching associations generated by the graph matching method may be unreliable because the images captured by different cameras in a camera network are seriously affected by the variations of the camera settings and illumination conditions. We introduce the indirect matching to assist the cross-view matching and obtain more reliable matches by considering the similarity relationships across a camera network. Specifically, given the initial cross-camera matching configuration in a camera network $\mathbf{X} = \{X_{p,q} | p, q = 1, 2, \dots, R, p < q\}$ generated by the bipartite graph matching method, we can further derive a new indirect pairwise matching $X'_{p,q}$ for each original matching association matrix $X_{p,q}$ by the composition of a few assignment matrices $X'_{p,q} = X_{p,r_1} X_{r_1,r_2} \dots X_{r_n,q}$, where $p, q, r_1, r_2, \dots, r_n$ are cameras in the same camera network and $p, q \neq r_1, r_2, \dots, r_n$ [35]. Consequently, for a pair of images $(\mathcal{P}_p^i, \mathcal{P}_q^j)$ captured from camera pairs (p, q) , we can obtain their matching association $x_{p,q}^{i,j}$ from the direct assignment matrix $X_{p,q}(i, j)$ and indirect assignment matrix $X'_{p,q}(i, j)$, where $X'_{p,q}(i, j) = x_{p,r_1}^{i,k_1} x_{r_1,r_2}^{k_1,k_2} \dots x_{r_n,q}^{k_n,j}$.

2) *Loop consistent matching*: Given two vertices \mathcal{P}_p^i and \mathcal{P}_q^j , it can be noted that for consistency, logical ‘AND’ relationship between the association value $x_{p,q}^{i,j}$ and the set of association values $\{x_{p,r_1}^{i,k_1}, x_{r_1,r_2}^{k_1,k_2}, \dots, x_{r_n,q}^{k_n,j}\}$ across possible vertices in the different cameras has to be maintained. In other words, the association value $x_{p,q}^{i,j}$ between the two vertices \mathcal{P}_p^i and \mathcal{P}_q^j has to be 1, and it has to satisfy the indirect matching association $x_{p,r_1}^{i,k_1} x_{r_1,r_2}^{k_1,k_2} \dots x_{r_n,q}^{k_n,j} = 1$. In [23], [24], it has been proven that if the loop consistent constraint is satisfied for every triplet of cameras, it automatically ensures consistency for every possible combination of cameras taking 3 or more of them. Thus, the consistent matching pair \mathcal{P}_p^i and \mathcal{P}_q^j in the network of cameras has to satisfy the direct cross-view matching association $x_{p,q}^{i,j} = 1$ and a person k in camera r should satisfy: $x_{p,r}^{i,k} x_{k,q}^{k,j} = 1$ as shown in Figure 3(a). We formulate it as follows.

$$x_{p,q}^{i,j} = 1 \text{ and } \exists \mathcal{P}_r^k, x_{p,r}^{i,k} x_{k,q}^{k,j} = 1, r \neq p, q \quad (5)$$

We can see that loop consistent matches not only satisfy the direct pairwise matching, but also the indirect matching.

3) *Transitive inference consistent matching*: Transitive inference among person identities across multiple cameras and their logical consequences are strongly informative properties [32]. We exploit the transitive relations for enhancing the

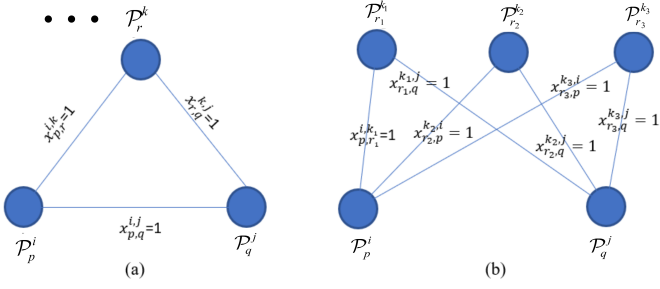


Fig. 3. Loop consistency and transitive inference consistency for the estimation of the reliable cross-camera image pairs. (a) illustrates the loop consistent constraints. If $x_{p,q}^{i,j} = 1$ and the exiting person k in camera r satisfies $x_{p,r}^{i,k} x_{r,q}^{k,j} = 1$, then the matching $(\mathcal{P}_p^i, \mathcal{P}_q^j)$ is reliable. (b) shows the reliability of the transitive inference pairs selection. Larger RT value indicates more reliability of the transitive inference-based matching pairs

performance of the cross-view matching. To illustrate the idea, let us consider a plausible scenario as shown in Figure 3(b). If we know from the bipartite graph matching across camera pairs that pairs $(\mathcal{P}_p^i, \mathcal{P}_r^k)$ and $(\mathcal{P}_r^k, \mathcal{P}_q^j)$ have positive matching association, then according to the transitive inference we can directly infer that $(\mathcal{P}_p^i, \mathcal{P}_q^j)$ also have the same identity, i.e., $x_{p,r}^{i,k} x_{r,q}^{k,j} = 1 \Rightarrow x_{p,q}^{i,j} = 1$. By introducing transitivity, we can increase the number of matching pairs through indirect inference. Usually, in a camera network, with more than three cameras, we define the reliability of the transitive inference-based cross-view matching across a camera network

$$\text{RT}_{p,q}^{i,j} = \sum_r \sum_{k=1}^{n_r} x_{p,r}^{i,k} x_{r,q}^{k,j}, r \neq p, q \quad (6)$$

where p, q and r are cameras in a network, and $r \neq p, r \neq q$. n_r is the number of persons captured in camera r . $\text{RT}_{p,q}^{i,j}$ denotes the reliability of the transitive inference-based cross-camera matching $(\mathcal{P}_p^i, \mathcal{P}_q^j)$. The larger the value RT is, the more reliable the transitive matching is, as shown in Figure 3(b), i.e. $\text{RT}_{p,q}^{i,j} = 3$. When the reliability value $\text{RT}_{p,q}^{i,j}$ satisfies $\text{RT}_{p,q}^{i,j} > 1$, we regard the matching pair $(\mathcal{P}_p^i, \mathcal{P}_q^j)$ as a transitive inference consistent matching.

In a camera network, we regard a cross-view matching pair as a reliable matching when it satisfies the loop consistency or transitive inference consistency. Furthermore, combining loop consistency and transitive inference consistency, we define a metric for measuring the reliability of cross-camera matched image pairs as follows:

$$\text{RLT}_{p,q}^{i,j} = x_{p,q}^{i,j} + \sum_r \sum_{k=1}^{n_r} x_{p,r}^{i,k} x_{r,q}^{k,j}, r \neq p, q, \quad (7)$$

where $\text{RLT}_{p,q}^{i,j}$ represents the reliability of the cross-view matched image pair $(\mathcal{P}_p^i, \mathcal{P}_q^j)$. With the increase in RLT value, the obtained matches are more and more reliable, however, the number of the obtained image pairs are less. Therefore, we need to adjust the reliability value for balancing the performance between the quality and quantity of the cross-view matched image pairs.

C. Iterative Updating

Different cameras have different settings and the captured images are seriously affected by variability in illumination conditions, camera viewing angles, and background clutter[13]. So, a fixed matching cost matrix constructed in the original feature space usually does not produce satisfactory recognition performance and hence it is not suitable in many person re-identification systems. Following [21], [22], we embed our method into an iterative updating framework to refine the matching cost matrix. Specifically, we introduce an iterative framework which iterates between the consistent cross-view matching and distance metric learning as shown in Figure 2. In each iteration, we first construct a bipartite graph for each camera pair and then select the reliable image pairs using the consistent constraints. Finally, a set of discriminative pair-wise distance metric are learned using the corresponding reliable image pairs. The alternating procedure ensures that the matched image pairs gradually become more accurate, and the learned metrics models become more discriminative.

IV. EXPERIMENTAL RESULTS

A. Experimental Setting

1) *Datasets*: We use three publicly available person re-identification datasets for experiments such as MARS and Market1501 dataset which are captured by 6 cameras in a university campus, and DukeMTMC-VideoReID dataset which is captured by 8 synchronized cameras. While **MARS**[36] is a large-scale video-based re-id dataset containing 17,503 video tracklets of 1,261 identities, **Market-1501**[37] is a large-scale image-based re-id dataset that contains 32,668 images of 1,501 identities. On the other hand, **DukeMTMC-VideoReID** is a large-scale video-based re-id dataset derived from the DukeMTMC dataset [38] that contains 4,832 tracklets of 1,404 identities. More details on the datasets are shown in Table I.

2) *Feature extraction*: We use both hand-crafted feature designed for person re-id (LOMO feature) [14] and deep convolutional neural network (CNN) features for evaluating the performance of our proposed method. The LOMO feature descriptor is of 26,960 dimensions. For the LOMO feature, we use the principal component analysis (PCA) method to reduce the dimension to 600. For the deep CNN feature, we first utilize a pre-trained ResNet50 model [39] to extract the features as in [15] and then ℓ_2 normalize it for all the experiments. For video-based datasets, each tracklet is regarded as an individual sample and we conduct max-pooling for each sample to get more robust video feature representation.

3) *Evaluation metrics*: We follow the standard training/testing split [36], [37], [38]. We use 625 identities for training and the remaining 636 identities for testing in MARS dataset. For Market1501 dataset, we use 12,936 images of 751 identities for training and 19,732 images of 750 identities for testing. We use 2,196 tracklets of 702 identities for training, 2,636 tracklets of other 702 identities for testing in DukeMTMC-VideoReID dataset. We utilize the Cumulative Matching Characteristic (CMC) curve and the mean average precision (mAP) to evaluate the recognition performance of each method. We report the Rank-1, Rank-5, Rank-10 scores

TABLE I
THE NUMBER OF IDENTITIES CAPTURED BY EACH CAMERA ON THE TRAINING SET OF THREE DATASETS

Dataset	Index	CAM1	CAM2	CAM3	CAM4	CAM5	CAM6	CAM7	CAM8
Market1501	#ID	652	541	694	241	576	558	-	-
MARS	#ID	520	447	314	195	375	104	-	-
DukeMTMC-VideoReID	#ID	404	378	201	165	218	348	217	265

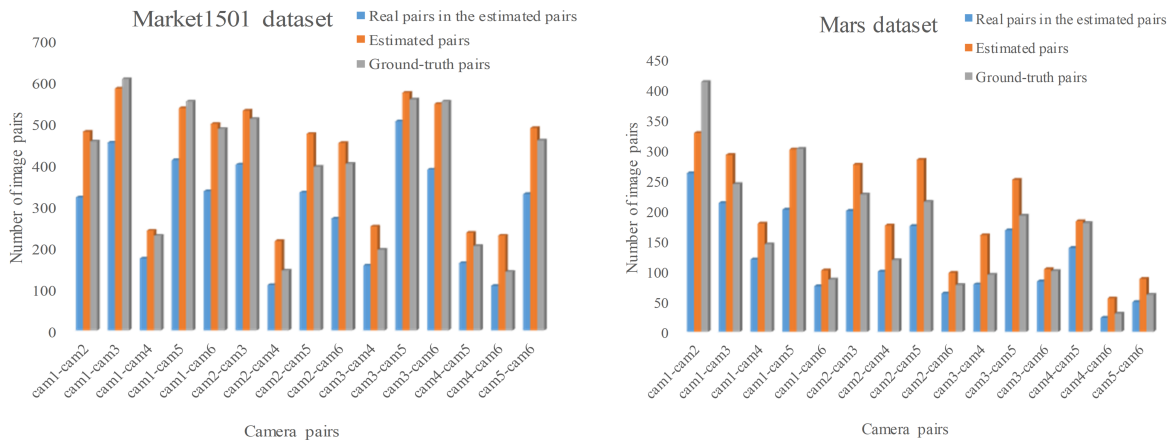


Fig. 4. Consistent cross-view matching performance across pair of cameras on Market1501 dataset and MARS dataset.

to represent the CMC curve. Note that our method does not use any labeled samples for model initialization or training.

4) *Implementation details:* In this paper, we employ Hungarian algorithm to solve the cross-view matching problem and we adopt the distance metric learning (MLAPG)[40] approach for matching persons in re-id. Note that our approach is not specific to any type of matching and metric learning algorithm used for person re-id. During training, we train a metric learning model for each pair of cameras using the reliable image pairs from the corresponding camera pairs and in testing, we measure each query-gallery pair using all the learned metric models to mitigate the insufficient image pairs across cameras and the minimum value is regarded as the final recognition result for each pair. We iteratively update the cross-view matching and metric learning for 10 iterations in all our experiments. All the reported results are based on the reliability value of the consistent cross-view matching $RLT > 1$ and deep CNN features.

B. Evaluating Cross-view Image Pairs Matching

We use the standard precision, recall and F-score to illustrate the performance of cross-view image pairs matching across a camera network. The results on Market1501, MARS and DukeMTMC-VideoReID datasets are shown in Table II. From Table II, we can see that using our method, 70.4% of the matched image pairs are the correct matches on Market1501 dataset (72.3% on MARS dataset) and 75.6% of the correct cross-view matched image pairs are among the true matches on Market1501 dataset (76.8% on MARS dataset). We also measure the performance on a larger camera network DukeMTMC-VideoReID dataset where it is hard to obtain efficient cross-view matches as the persons appearing

TABLE II
PERFORMANCE OF CROSS-VIEW IMAGE PAIR MATCHING ON MARKET1501 DATASET, MARS DATASET AND DUKEMTMC-VIDEOREID DATASET. PRECISION, RECALL AND F-SCORE (%) ARE REPORTED

Dataset	Precision	Recall	F-score
Market1501	70.4	75.6	72.9
MARS	72.3	76.8	74.5
DukeMTMC-VideoReID	50.9	55.0	52.9

in different cameras are very different. For example, there is only one person who appears in both camera 4 and camera 7. From Table II, we can see that our method still achieves 50.9% matching precision and obtains 55.0% of the real cross-view image pairs among all the true matches with $RLT > 2$ on this challenging dataset.

We further demonstrate the details on the cross-camera matching performance on Market1501 dataset and MARS dataset in Figure 4. From the figure, We can see that different cameras capture very different person identities. By using our method, we can obtain most correct matches and reject the false positive matches. For example, camera 1 captures 652 different persons and camera 4 captures 241 persons on Market1501 dataset, that means there are at least 411 outliers will affect the matching performance. However, from Figure 4, we can see that based on our method we can obtain 240 matches including 173 matches among 228 ground-truth matches. This again shows that our method is very efficient for cross-camera label estimation in a network of cameras.

TABLE III
RECOGNITION PERFORMANCE WITH (/WITHOUT) CROSS-VIEW DISTANCE
METRIC LEARNING. RANK-K ACCURACY (%) AND mAP (%) ARE
REPORTED.

MARS	R1	R5	R10	mAP
OURS w/o cross-view ML	62.1	75.1	79.1	38.5
OURS w cross-view ML	63.7	76.2	80.0	42.1
Market1501	R1	R5	R10	mAP
OURS w/o cross-view ML	70.6	83.1	88.2	40.5
OURS w cross-view ML	71.7	83.6	88.4	43.1
DukeMTMC-VideoReID	R1	R5	R10	mAP
OURS w/o cross-view ML	73.6	87.1	90.2	65.5
OURS w cross-view ML	75.4	87.3	90.9	67.0

w cross-view ML: with cross-view metric learning. w/o cross-view ML: training a distance metric model for one dataset (without cross-view metric learning).

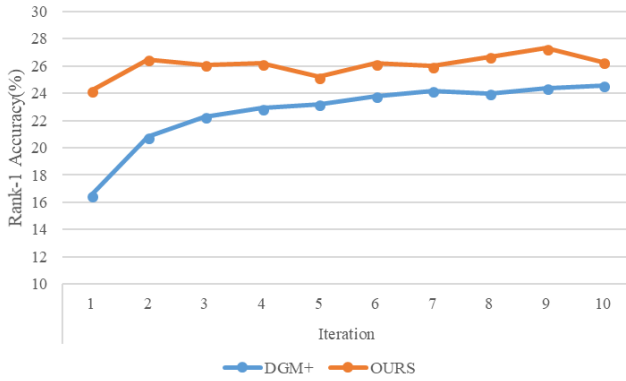


Fig. 5. Rank-1 accuracy of the proposed method and DGM+ on MARS dataset with the same LOMO feature at each iteration.

C. Evaluating Cross-view Metric Learning

In the proposed consistent cross-view matching framework, we train a separate distance metric model for each pair of cameras. To evaluate the advantages of this method, we demonstrate the recognition performance by comparing the results of the proposed method by comparing with a single metric model trained using the entire dataset.

From Table III, we can see that in our framework, by the using of the cross-view distance metric learning, the recognition performance can be improved compared with the strategy of training a single distance metric model for the entire dataset, especially for the mAP value. Specifically, for MARS dataset, we improve 1.6% and 3.6% for rank-1 score and mAP respectively. For Market1501 dataset and DukeMTMC-VideoReID dataset, the rank-1 accuracy increases by 1.1% and 1.8%, and mAP value increases by 2.6% and 1.5%, respectively. The cross-view distance metric learning across each pair of cameras help to reduce the negative effect caused by the variance between cameras by to some extent. Moreover, in the testing procedure, to mitigate the problem of the insufficient matched image pairs across cameras, we measure each query-gallery pair using all of the learned metric models and the minimum value is regarded as the final recognition result.

D. Evaluation of Iterative Updating

Motivated by [21], [22], we embed our consistent cross-view matching approach into an iterative updating framework which iterates between the consistent cross-view matching and the cross-view distance metric learning. We compare the recognition performance of the proposed method and DGM+ method in [22] using the LOMO features under different iterations. Figure 5 reports the rank-1 accuracy of these two methods on MARS dataset. We can see that our method outperforms DGM+ consistently with the best recognition performance of 27.5% at 9th iteration. As expected, with the the increase in number of iterations, we can obtain more and more reliable cross-camera matched image pairs and the learned metric models become more and more robust.

E. Evaluating Recognition Performance under Different Reliability (RLT) Values

The quality and quantity of the estimated pair-wise labels are very important for distance metric learning and recognition process in unsupervised person re-id. Both of them are related to the reliability value (RLT value) of the cross-view matched image pairs. Thus, we compare the recognition performance under different reliability values to select the optimal one. We use rank-1 accuracy and mAP under 5 different reliability values (RLT) where $RLT = 0$ denotes that we measure the recognition performance using Euclidean distance directly without the consistent cross-view matching and distance metric learning method. From Table IV, we can see that the recognition performance fluctuates a little with the increase in RLT values. The fluctuation is caused by the trade-off between the number of matched image pairs and the reliability of the matched pairs. At the beginning, by the using of our method, we can collect the most cross-view matched image pairs, but it also introduces massive false positive pairs. After that, although the number of matched image pairs declines, the reliability of the matching increases. We onbserve that with $RLT > 1$, we obtain the best recognition performance with rank-1=63.7%, mAP=42.1% on MARS dataset (rank-1=71.7 and mAP=43.1% on Market1501 dataset) which balances the quality and quantity of the matched image pairs. Similarly, for DukeMTMC-VideoReID dataset, we obtain the best recognition performance at $RLT > 2$ with rank-1=75.4 and mAP=67.0, respectively.

F. Comparison with the State-of-the-art Unsupervised Person Re-identification Methods

In this section, we compare our method with some representative state-of-the-art unsupervised person re-identification methods on three different datasets.

MARS. We compare our approach with 8 different unsupervised methods that fall into two main categories: (1) methods based on handcrafted features such as GRDL [41], UnKISS [42], DGM+ [22] using LOMO feature, and (2) methods based on deep learning features such as DGM+ [22] using deep IDE features, OIM [25], Stepwise [26], RACE [43], DAL [44], BUC [15]. As can be seen from V, the proposed method

TABLE IV
RECOGNITION PERFORMANCE UNDER DIFFERENT RELIABILITY VALUE ON MARKET1501 DATASET, MARS DATASET AND DUKEMTMC-VIDEOREID DATASET. RANK-1 ACCURACY (%) AND MAP (%) ARE REPORTED.

Dataset	RLT=0		RLT>0		RLT>1		RLT>2		RLT>3	
	R1	mAP	R1	mAP	R1	mAP	R1	mAP	R1	mAP
MARS	61.1	38.0	62.6	37.9	63.7	42.1	62.8	40.8	60.3	40.3
Market1501	66.2	38.3	70.3	39.6	71.7	43.1	69.5	42.3	67.1	41.0
DukeMTMC-VideoReID	69.2	61.9	69.2	60.3	73.6	65.7	75.4	67.0	74.8	67.5

RLT =0 denotes that we measure the performance using Euclidean distance in testing procedure without cross-view matching and distance metric learning.

TABLE V
COMPARISON WITH STATE-OF-THE-ART UNSUPERVISED PERSON RE-IDENTIFICATION METHOD ON MARS DATASET RANK-K ACCURACY (%) AND MAP (%) ARE REPORTED.

Methods	R1	R5	R10	mAP
GRDL [41]	19.3	33.2	41.6	9.6
UnKISS [42]	22.3	37.4	47.2	10.6
DGM+LOMO [22]	24.7	39.4	47.0	11.7
OURS+LOMO	27.6	43.7	50.3	12.5
OIM [25]	33.7	48.1	54.8	13.5
Stepwise [26]	41.2	55.5	-	19.6
RACE [43]	43.2	57.1	62.1	24.5
DGM+IDE [22]	48.1	64.7	71.1	29.2
DAL [44]	49.3	65.9	72.2	23.0
BUC [15]	61.1	75.1	80.0	38.0
OURS	63.7	76.2	80.0	42.1

TABLE VI
COMPARISON WITH STATE-OF-THE-ART UNSUPERVISED PERSON RE-IDENTIFICATION METHOD ON MARKET1501 DATASET. RANK-K ACCURACY (%) AND MAP (%) ARE REPORTED

Methods	R1	R5	R10	mAP
BOW [37]	35.8	52.4	60.3	14.8
OIM [25]	38.0	58.0	66.3	14.0
UMDL [45]	34.5	52.6	59.6	12.4
PUL [16]	44.7	59.1	65.6	20.1
EUG [38]	49.8	66.4	72.7	22.5
CAMEL [46]	54.5	-	-	26.3
SPGAN [47]	58.1	76.0	82.7	26.7
TJ-AIDL [48]	58.2	-	-	26.5
DGM+IDE [22]	57.6	-	-	31.2
BUC [15]	66.2	79.6	84.5	38.3
OURS	71.7	83.6	88.4	43.1

TABLE VII
COMPARISON WITH STATE-OF-THE-ART UNSUPERVISED PERSON RE-IDENTIFICATION METHOD ON DUKEMTMC-VIDEOREID DATASET. RANK-K ACCURACY (%) AND MAP (%) ARE REPORTED

Methods	R1	R5	R10	mAP
OIM [25]	51.1	70.5	76.2	43.8
DGM+IDE [22]	42.3	57.9	69.3	33.6
Stepwise [26]	56.2	70.3	79.2	46.7
EUG [38]	72.7	84.1	-	63.2
BUC [15]	69.2	81.1	85.8	61.9
OURS	75.4	87.3	90.9	67.0

significantly outperforms all the compared methods under the handcrafted feature setting. Compared to DGM+, we achieve 2.9 points and 0.8 points improvement using the same LOMO feature in rank-1 accuracy and mAP, respectively. Similarly, our method also obtains the best recognition performance 63.7% for rank-1 and 42.1% for mAP while comparing with deep learning based alternatives. As expected, the proposed method performs the best while using deep CNN feature compared to the handcrafted LOMO features.

Market1501. We compare our proposed method with 10 different unsupervised person re-identification methods, such as BOW [37], OIM [25], UMDL [45], PUL [16], EUG [38], CAMEL [46], SPGAN [47], TJ-AIDL [48], DGM+ [22], BUC [15]. Most of the results in Table VI are from [15], [22]. Our method significantly outperforms all the other compared methods with rank-1 accuracy of 71.1% and mAP of 43.1%. Among the alternatives, the most recent BUC is the most competitive. However, we achieve 5.5 points and 4.8 points improvement in rank-1 accuracy and mAP, respectively over the BUC method. This significant improvement contributes to the consistent cross-view matching that exploits similarity relationships across pair of cameras, and the specific distance metric models learned for each camera pair in a camera network. Compared to DGM+ which utilizes a part of labeled images for initializing the model, our method employs an unsupervised feature embedding learning method and by introducing consistent constraints, we can obtain better recognition performance over the DGM+ method.

DukeMTMC-VideoReID. We also evaluate our method on a larger camera network captured by 8 different cameras by comparing with 5 state-of-the-art methods such as OIM [25], DGM+ [22], Stepwise [26], EUG [38], BUC [15]. Results in Table VII illustrate the superiority of the proposed unsupervised framework over all the compared methods. We achieve the best recognition performance with rank-1 accuracy of 75.4% and mAP of 67.0% with RLT > 2, respectively.

G. Ablation Studies

To better evaluate the effectiveness of our proposed method, we conduct ablation studies using DukeMTMC-VideoReID and Market1501 datasets with different combinations of our proposed approach. As shown in Table VIII, Baseline denotes that we measure the recognition performance using the Euclidean distance *without* considering the similarity information of the cross-view image pairs. At first, we show the effect of the cross-view matching (CM) by introducing the graph

TABLE VIII
METHODS COMPARISON WHEN TESTED ON DUKEMTMC-VIDEOREID DATASET, MARKET1501 DATASET WITH (/WITHOUT) CONSISTENT SIMILARITY INFORMATION. RANK-K ACCURACY (%) AND mAP (%) ARE REPORTED.

DukeMTMC-VideoReID	R1	R5	R10	mAP
Baseline	69.2	81.1	85.8	61.9
Ours w CM	72.2	86.2	89.3	64.3
Ours w CM+LC	73.9	87.8	90.7	66.1
Ours w CM+LC+TRC	75.4	87.3	90.9	67.0
Market1501	R1	R5	R10	mAP
Baseline	66.2	79.6	84.5	38.3
Ours w CM	71.2	83.6	88.3	42.3
Ours w CM+LC	71.0	83.7	88.6	42.5
Ours w CM+LC+TRC	71.7	83.6	88.4	43.1

Baseline: we measure the recognition performance using the Euclidean distance directly without considering the cross-view image pairs similarity information. w/CM: Cross-view matching by introducing the graph matching method into baseline. LC: loop consistent constraints. TRC: transitive inference consistent constraints.

matching method into the baseline to take the similarity information across camera pairs into account. For DukeMTMC-VideoReID dataset, we can see that “Ours w/CM” improves the recognition performance from 69.2% to 72.2% for rank-1 accuracy and 61.9% to 64.3% for mAP, respectively. This demonstrates that the cross-view matching is an effective way to improve the recognition performance by exploiting the similarity relationships across camera pairs. Furthermore, we validate the effect caused by the loop consistent constraints (LC) and transitive inference constraints (TRC), respectively. As shown in Table VIII, by introducing the consistent constraints, the recognition performance is improved consistently. For example, “Ours w/CM+LC” improves the recognition performance from 72.2% to 73.9% for rank-1 accuracy and 64.3% to 66.1% for mAP, respectively, by selecting reliable image pairs from all estimated matches. Finally, when integrating the transitive inference consistent constraints, “Ours w/CM+LC+TRC” achieves the best recognition performance with rank-1 accuracy of 75.4% and mAP of 67.0% respectively on the DukeMTMC-VideoReID dataset.

Similarly for Market1501, we also observe that by introducing the consistent cross-view similarity information the recognition performance is improved by a large margin. As shown in Table VIII, after we introduce the cross-view similarity information, the recognition accuracy improves 5 points and 4 points for rank-1 accuracy and mAP, respectively. By integrating the consistent constraints into the cross-view matching, the recognition performance is improved from 71.2% to 71.7% for rank-1 accuracy and 42.3% to 43.1% for mAP.

V. CONCLUSIONS

In this paper, we propose a consistent cross-view matching framework to address the unsupervised person re-identification task by exploiting more reliable image pairs across camera pairs. We first introduce loop consistent and transitive inference consistent constraints into cross-view matching, which will reduce the contradictory matches the matched results

from different camera pairs are combined. We then present a definition of cross-view matching reliability which will help us to select image pairs in an effective way by balancing the performance between the quality and quantity of the estimated matches. Finally, we embed our method into an iterative framework to jointly optimize the learned cross-view matches and the distance metric models. Rigorous experiments on three standard person re-identification datasets show the advantage of our approach over the state-of-the-art methods.

ACKNOWLEDGMENT

This research is supported by China Scholarship Council and the National Natural Science Foundation of China under Grant No. 61771189.

REFERENCES

- [1] L. Zheng, Y. Yang, and Q. Tian, “Sift meets cnn: A decade survey of instance retrieval,” *IEEE transactions on pattern analysis and machine intelligence*, vol. 40, no. 5, pp. 1224–1244, 2017.
- [2] Y. Sun, L. Zheng, Y. Yang, Q. Tian, and S. Wang, “Beyond part models: Person retrieval with refined part pooling (and a strong convolutional baseline),” in *Proceedings of the European Conference on Computer Vision (ECCV)*, 2018, pp. 480–496.
- [3] J. Lin, L. Ren, J. Lu, J. Feng, and J. Zhou, “Consistent-aware deep learning for person re-identification in a camera network,” in *Proceedings of the IEEE conference on computer vision and pattern recognition*, 2017, pp. 5771–5780.
- [4] G. Chen, J. Lu, M. Yang, and J. Zhou, “Spatial-temporal attention-aware learning for video-based person re-identification,” *IEEE Transactions on Image Processing*, 2019.
- [5] L. Ren, J. Lu, J. Feng, and J. Zhou, “Uniform and variational deep learning for rgb-d object recognition and person re-identification,” *IEEE Transactions on Image Processing*, 2019.
- [6] X. Chang, T. M. Hospedales, and T. Xiang, “Multi-level factorisation net for person re-identification,” in *Proceedings of the IEEE Conference on Computer Vision and Pattern Recognition*, 2018, pp. 2109–2118.
- [7] D. Chen, H. Li, X. Liu, Y. Shen, J. Shao, Z. Yuan, and X. Wang, “Improving deep visual representation for person re-identification by global and local image-language association,” in *Proceedings of the European Conference on Computer Vision (ECCV)*, 2018, pp. 54–70.
- [8] J. Si, H. Zhang, C.-G. Li, J. Kuen, X. Kong, A. C. Kot, and G. Wang, “Dual attention matching network for context-aware feature sequence based person re-identification,” in *Proceedings of the IEEE Conference on Computer Vision and Pattern Recognition*, 2018, pp. 5363–5372.
- [9] C. Su, J. Li, S. Zhang, J. Xing, W. Gao, and Q. Tian, “Pose-driven deep convolutional model for person re-identification,” in *Proceedings of the IEEE International Conference on Computer Vision*, 2017, pp. 3960–3969.
- [10] Y. Suh, J. Wang, S. Tang, T. Mei, and K. Mu Lee, “Part-aligned bilinear representations for person re-identification,” in *Proceedings of the European Conference on Computer Vision (ECCV)*, 2018, pp. 402–419.
- [11] G. Wang, Y. Yuan, X. Chen, J. Li, and X. Zhou, “Learning discriminative features with multiple granularities for person re-identification,” in *2018 ACM Multimedia Conference on Multimedia Conference*. ACM, 2018, pp. 274–282.
- [12] Y. Wang, L. Wang, Y. You, X. Zou, V. Chen, S. Li, G. Huang, B. Hariharan, and K. Q. Weinberger, “Resource aware person re-identification across multiple resolutions,” in *Proceedings of the IEEE Conference on Computer Vision and Pattern Recognition*, 2018, pp. 8042–8051.
- [13] L. Ma, X. Yang, and D. Tao, “Person re-identification over camera networks using multi-task distance metric learning,” *IEEE Transactions on Image Processing*, vol. 23, no. 8, pp. 3656–3670, 2014.
- [14] S. Liao, Y. Hu, X. Zhu, and S. Z. Li, “Person re-identification by local maximal occurrence representation and metric learning,” in *Proceedings of the IEEE conference on computer vision and pattern recognition*, 2015, pp. 2197–2206.
- [15] Y. Lin, X. Dong, L. Zheng, Y. Yan, and Y. Yang, “A bottom-up clustering approach to unsupervised person re-identification,” in *AAAI Conference on Artificial Intelligence*, vol. 2, 2019.

- [16] H. Fan, L. Zheng, C. Yan, and Y. Yang, "Unsupervised person re-identification: Clustering and fine-tuning," *ACM Transactions on Multimedia Computing, Communications, and Applications (TOMM)*, vol. 14, no. 4, p. 83, 2018.
- [17] H.-X. Yu, W.-S. Zheng, A. Wu, X. Guo, S. Gong, and J.-H. Lai, "Unsupervised person re-identification by soft multilabel learning," *arXiv preprint arXiv:1903.06325*, 2019.
- [18] M. Li, X. Zhu, and S. Gong, "Unsupervised person re-identification by deep learning tracklet association," in *Proceedings of the European Conference on Computer Vision (ECCV)*, 2018, pp. 737–753.
- [19] R. Zhao, W. Ouyang, and X. Wang, "Unsupervised salience learning for person re-identification," in *Proceedings of the IEEE Conference on Computer Vision and Pattern Recognition*, 2013, pp. 3586–3593.
- [20] E. Kodirov, T. Xiang, and S. Gong, "Dictionary learning with iterative laplacian regularisation for unsupervised person re-identification." in *BMVC*, vol. 3, 2015, p. 8.
- [21] M. Ye, A. J. Ma, L. Zheng, J. Li, and P. C. Yuen, "Dynamic label graph matching for unsupervised video re-identification," in *Proceedings of the IEEE International Conference on Computer Vision*, 2017, pp. 5142–5150.
- [22] M. Ye, J. Li, A. J. Ma, L. Zheng, and P. C. Yuen, "Dynamic graph co-matching for unsupervised video-based person re-identification," *IEEE Transactions on Image Processing*, 2019.
- [23] A. Das, A. Chakraborty, and A. K. Roy-Chowdhury, "Consistent re-identification in a camera network," in *European conference on computer vision*. Springer, 2014, pp. 330–345.
- [24] A. Chakraborty, A. Das, and A. K. Roy-Chowdhury, "Network consistent data association," *IEEE transactions on pattern analysis and machine intelligence*, vol. 38, no. 9, pp. 1859–1871, 2015.
- [25] T. Xiao, S. Li, B. Wang, L. Lin, and X. Wang, "Joint detection and identification feature learning for person search," in *Proceedings of the IEEE Conference on Computer Vision and Pattern Recognition*, 2017, pp. 3415–3424.
- [26] Z. Liu, D. Wang, and H. Lu, "Stepwise metric promotion for unsupervised video person re-identification," in *Proceedings of the IEEE International Conference on Computer Vision*, 2017, pp. 2429–2438.
- [27] Z. Zhong, L. Zheng, Z. Luo, S. Li, and Y. Yang, "Invariance matters: Exemplar memory for domain adaptive person re-identification," in *Proceedings of the IEEE Conference on Computer Vision and Pattern Recognition*, 2019, pp. 598–607.
- [28] Y. Choi, M. Choi, M. Kim, J.-W. Ha, S. Kim, and J. Choo, "Stargan: Unified generative adversarial networks for multi-domain image-to-image translation," in *Proceedings of the IEEE Conference on Computer Vision and Pattern Recognition*, 2018, pp. 8789–8797.
- [29] Z. Zhong, L. Zheng, Z. Zhong, S. Li, and Y. Yang, "Camera style adaptation for person re-identification," in *Proceedings of the IEEE Conference on Computer Vision and Pattern Recognition*, 2018, pp. 5157–5166.
- [30] A. C. Berg, T. L. Berg, and J. Malik, "Shape matching and object recognition using low distortion correspondences," in *CVPR (1)*. Citeseer, 2005, pp. 26–33.
- [31] Z. Zhang, Q. Shi, J. McAuley, W. Wei, Y. Zhang, and A. Van Den Hengel, "Pairwise matching through max-weight bipartite belief propagation," in *Proceedings of the IEEE Conference on Computer Vision and Pattern Recognition*, 2016, pp. 1202–1210.
- [32] S. Roy, S. Paul, N. E. Young, and A. K. Roy-Chowdhury, "Exploiting transitivity for learning person re-identification models on a budget," in *Proceedings of the IEEE Conference on Computer Vision and Pattern Recognition*, 2018, pp. 7064–7072.
- [33] D. Li, W.-C. Hung, J.-B. Huang, S. Wang, N. Ahuja, and M.-H. Yang, "Unsupervised visual representation learning by graph-based consistent constraints," in *European Conference on Computer Vision*. Springer, 2016, pp. 678–694.
- [34] Y. Shen, W. Lin, J. Yan, M. Xu, J. Wu, and J. Wang, "Person re-identification with correspondence structure learning," in *Proceedings of the IEEE International Conference on Computer Vision*, 2015, pp. 3200–3208.
- [35] J. Yan, M. Cho, H. Zha, X. Yang, and S. M. Chu, "Multi-graph matching via affinity optimization with graduated consistency regularization," *IEEE transactions on pattern analysis and machine intelligence*, vol. 38, no. 6, pp. 1228–1242, 2015.
- [36] L. Zheng, Z. Bie, Y. Sun, J. Wang, C. Su, S. Wang, and Q. Tian, "Mars: A video benchmark for large-scale person re-identification," in *European Conference on Computer Vision*. Springer, 2016, pp. 868–884.
- [37] L. Zheng, L. Shen, L. Tian, S. Wang, J. Wang, and Q. Tian, "Scalable person re-identification: A benchmark," in *Proceedings of the IEEE International Conference on Computer Vision*, 2015, pp. 1116–1124.
- [38] Y. Wu, Y. Lin, X. Dong, Y. Yan, W. Ouyang, and Y. Yang, "Exploit the unknown gradually: One-shot video-based person re-identification by stepwise learning," in *Proceedings of the IEEE Conference on Computer Vision and Pattern Recognition*, 2018, pp. 5177–5186.
- [39] K. He, X. Zhang, S. Ren, and J. Sun, "Deep residual learning for image recognition," in *Proceedings of the IEEE conference on computer vision and pattern recognition*, 2016, pp. 770–778.
- [40] S. Liao and S. Z. Li, "Efficient psd constrained asymmetric metric learning for person re-identification," in *Proceedings of the IEEE International Conference on Computer Vision*, 2015, pp. 3685–3693.
- [41] E. Kodirov, T. Xiang, Z. Fu, and S. Gong, "Person re-identification by unsupervised ℓ_1 graph learning," in *European conference on computer vision*. Springer, 2016, pp. 178–195.
- [42] F. M. Khan and F. Bremond, "Unsupervised data association for metric learning in the context of multi-shot person re-identification," in *2016 13th IEEE International Conference on Advanced Video and Signal Based Surveillance (AVSS)*. IEEE, 2016, pp. 256–262.
- [43] X. L. Ye, M. and P. C. Yuen, "Robust anchor embedding for unsupervised video person re-identification in the wild," in *European conference on computer vision*. Springer, 2018, pp. 170–186.
- [44] Y. Chen, X. Zhu, and S. Gong, "Deep association learning for unsupervised video person re-identification," *arXiv preprint arXiv:1808.07301*, 2018.
- [45] P. Peng, T. Xiang, Y. Wang, M. Pontil, S. Gong, T. Huang, and Y. Tian, "Unsupervised cross-dataset transfer learning for person re-identification," in *Proceedings of the IEEE conference on computer vision and pattern recognition*, 2016, pp. 1306–1315.
- [46] H.-X. Yu, A. Wu, and W.-S. Zheng, "Cross-view asymmetric metric learning for unsupervised person re-identification," in *Proceedings of the IEEE International Conference on Computer Vision*, 2017, pp. 994–1002.
- [47] W. Deng, L. Zheng, Q. Ye, G. Kang, Y. Yang, and J. Jiao, "Image-image domain adaptation with preserved self-similarity and domain-dissimilarity for person re-identification," in *Proceedings of the IEEE Conference on Computer Vision and Pattern Recognition*, 2018, pp. 994–1003.
- [48] J. Wang, X. Zhu, S. Gong, and W. Li, "Transferable joint attribute-identity deep learning for unsupervised person re-identification," in *Proceedings of the IEEE Conference on Computer Vision and Pattern Recognition*, 2018, pp. 2275–2284.